Molecular dynamics simulation of Eu^{3+}-doped chlorofluorozirconate glasses

1995 J. Phys.: Condens. Matter 7 4583

(http://iopscience.iop.org/0953-8984/7/24/001)

J. Phys.: Condens. Matter 7 (1995) 4583–4592. Printed in the UK

Molecular dynamics simulation of Eu^{3+}-doped chlorofluorozirconate glasses

M Takahashi, R Yamamoto, R Kanno and Y Kawamoto

Division of Science of Materials, Graduate School of Science and Technology, Kobe University, Nada, Kobe 657, Japan

Received 30 December 1994, in final form 20 March 1995

Abstract. Molecular dynamics simulations are performed for ZrF_4–BaF_2–EuF_3 glass systems in which 0, 5 and 10% F^- ions are substituted by Cl^- ions. Changes in local structures of the glasses around each cation are investigated in terms of increasing amount of substitutions of Cl^- for F^-. The average coordination number of F^- around Zr^{4+} is found to be approximately 7.7 and is independent of the amount of Cl^- substitution. The power spectra of the velocity autocorrelation functions are also calculated. The Zr–F stretching mode observed at around 800 cm^{-1} shows no shift with Cl^- substitution. These results show that the local structure around Zr^{4+} is not greatly affected by the small amount of Cl^- substitution. The F^- coordination number around Eu^{3+} at a radius of 3.0 Å and that around Ba^{2+} at a radius of 3.5 Å are found to decrease from 8.0 to 5.6 and from 9.2 to 5.1, respectively, as the Cl^- fraction increases. This means that Cl^- ions substituted for F^- exist almost around the Eu^{3+} or Ba^{2+} cation. Thus, even the small amount of Cl^- substitution greatly changes the local structures around Eu^{3+} and Ba^{2+}.

1. Introduction

The rare-earth-doped fluoride glasses (RDFG) have unique characteristics: high transmittance from the middle-infrared to the near-ultraviolet region [1], incorporation of rare-earth elements at high contents (up to 30 mol%) and low phonon energies [2]. RDFG have wide applications as optical devices such as laser oscillators and optical fibre amplifiers [3–5]. It is widely known that the optical properties of fluorescent ions doped in glasses are greatly affected by the structures of the glass host. Although many experimental studies have already been made on the structures of RDFGs [6–10], there are only a few studies which treat the fluorescence properties of rare-earth ions in RDFGs in terms of the glass structures except for the following studies: Adam *et al* [11] investigated the geometrics of Eu^{3+} in fluorozirconate glass using site-selective spectroscopy, Todoroki *et al* [12] reported the relationship between up-conversion luminescence of Er^{3+} and phonon energy around rare-earth ions, and Soga *et al* [13] studied the fluorescence properties of Eu^{3+} and local phonon modes around Eu^{3+} ions in ZrF_4-based glasses doped with Cl^-. These groups tried to relate the optical properties of RDFG and their structures.

Recent progress in computer systems makes it possible to investigate the microscopic structures of materials such as fluoride glasses by molecular dynamics (MD) or Monte Carlo (MC) simulation. MD and MC simulations have already been applied to many topics in the materials science field [14] and are regarded to be a powerful tool for understanding the microscopic structures and dynamics of materials. Hirao and Soga [15] have carried out MD simulations for borate glasses to investigate the local structures around Eu^{3+} ions in

0953-8984/95/244583+10$19.50

glasses. They found that profiles of Eu^{3+} fluorescence spectra are closely related to the local structures.

Previously, we have confirmed from experiments that the emission efficiencies of rare-earth ions in ZrF_4 glasses which contain a small amount of Cl^- ions as impurities are higher than those in pure ZrF_4 glasses [16]. Furthermore, Yano [17] reported that the substitution of Cl^- ions enhances the stabilities of the glasses, and Elyamani *et al* [18] reported that the absorption edge shifts to a longer wavelength with increasing amount of substitution of Cl^- for F^-. These findings are particularly of interest because they all suggest that the glass structures are greatly affected by a small amount of Cl^- substitution.

In the present study, we have performed MD simulations for ZrF_4–BaF_2–EuF_3 systems to investigate the changes in glass structures with increasing amount of Cl^- substitution for F^-. In particular, the local structures around each cation (Zr^{4+}, Eu^{3+} and Ba^{2+}) are extensively analysed by calculating the anion coordination numbers around the cation. The power spectra of velocity autocorrelation functions are calculated as well. The substitution of Cl^- is carried out up to 10% in total number of anions ([Cl]/([Cl] + [F]) × 100). This substitution range is within the experimentally obtained glass-forming range by means of a melting method.

2. Simulation methodology

In the present MD simulations, all ions interact through the Busing approximation of the Born–Mayer–Huggins type of potential without any dispersion terms. The potential energy (U_{ij}) between ions i and j is given by

$$U_{ij} = \frac{Z_i Z_j e^2}{r_{ij}} + f_0(b_i + b_j)\exp\left(\frac{a_i + a_j - r_{ij}}{b_i + b_j}\right)$$

where Z_i is the point charge located on the ion i, r_{ij} is the distance between ions i and j, $e = 1.6022 \times 10^{-19}$ C and $f_0 = 6.9472 \times 10^{-18}$ J. a_i and b_i are the size and softness parameters, which were empirically determined to reproduce the structures of various crystals containing the ion species at room temperature. The potential parameters used in the present calculations are listed in table 1. We have carried out MD simulations for three glass compositions $55ZrF_4$–$(35 - x)BaF_2$–$xBaCl_2$–$10EuF_3$ with $x = 0$, 8 and 16. These compositions correspond to 0, 5 and 10% Cl^- in the total anions. From now on, we refer these three glasses with $x = 0$, 8 and 16 as 0Cl, 5Cl and 10Cl, respectively. The unit cell contains 420 ions. The periodic boundary conditions are used as usual. The long-range corrections for potentials and forces due to the Coulomb term are treated by Ewald's [19] method. The temperatures and pressures are controlled by a simple scaling method. The initial ionic configurations were generated randomly; the initial velocities used were such that a Boltzmann distribution was followed at simulation temperatures. The equations of motion were integrated with a time step of 2.5 fs. The simulation schedule of each stage, i.e. equilibration, cooling, annealing and data analysis, is summarized in table 2.

The power spectra of the velocity autocorrelation functions for each ion are calculated using the MD data during 1600 steps after the annealing process. Bond angle distribution functions are also calculated by averaging over 3000 steps of MD data. In order to reduce statistical errors, simulations were carried out three times for each glass composition using different initial configurations.

Table 1. Potential parameters used for ZrF_4–BaF_2–$BaCl_2$–EuF_3 glasses.

Ion	Z	*a* (Å)	*b* (Å)
F^-	−1	1.500	0.090
Cl^-	−1	1.970	0.095
Zr^{4+}	+4	1.380	0.072
Ba^{2+}	+2	1.800	0.077
Eu^{3+}	+3	1.510	0.075

Table 2. Schedule of the present MD simulations.

Stage	Start step	End step	Temperature (K)	Cooling rate (K/step)
Equilibration	1	10000	2000	0
Cooling	10001	17000	2000–300	−1
Annealing	17001	27000	300	0
Data analyses	27001	31600	300	0

3. Results and discussion

3.1. Structure of Zr–Ba–Eu–F glass

Figure 1 shows a schematic diagram of the 55Zr–35Ba–10Eu–320F glass (0Cl) at 300 K. Zr–F and Eu–F bonds are shown by the solid lines. One can see that the network structures of ZrF_4 glasses are built up by linking ZrF_n(n = 7 or 8) polyhedra by edge or corner sharing. EuF_n polyhedra also play a part in building up the network. Ba^{2+} ions, however, are located in the interstitial positions of ZrF_n and EuF_n polyhedra which construct the three-dimensional network.

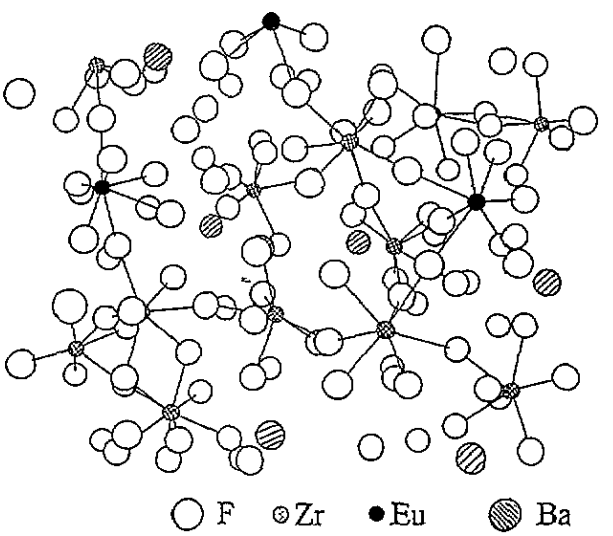

Figure 1. Schematic diagram of 55Zr–35Ba–10Eu–320F (0Cl) glass at 300 K.

3.2. Local structures around Zr^{4+}

The pair correlation functions $g_{Zr-X}(r)$ and the running coordination numbers $N_{Zr-X}(r)$ for the Zr^{4+}–X^- pair (X:F or Cl) are shown in figure 2. One can observe only very small peaks on the $g_{Zr-Cl}(r)$ curves in the r range from 2.5 to 3.0 Å for 5Cl and 10Cl. Thus we can say that very few Cl^- ions exist around Zr^{4+}. $g_{Zr-F}(r)$ curves show that the average interionic distances between Zr^{4+} and F^- are 2.10 Å and almost constant, being independent of the anion substitutions. As is observed on $N_{Zr-X}(r)$ curves in figure 2, the total anion coordination numbers around Zr^{4+} are about 7.7 in all glass compositions 0Cl, 5Cl and 10Cl. The curve profiles of $N_{Zr-X}(r)$ are quite similar to each other. Thus the average interionic distances between Zr^{4+} and F^-, and the total anion coordination numbers around Zr^{4+} are independent of the anion substitution.

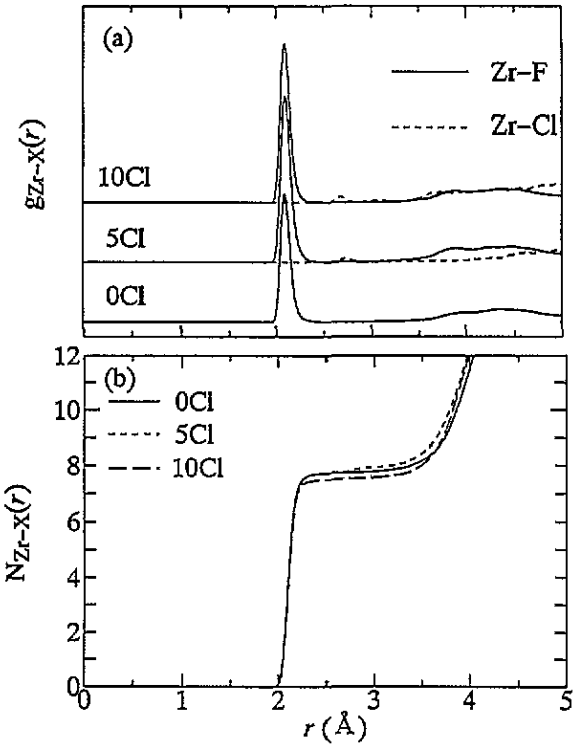

Figure 2. Pair correlation functions $g_{Zr-X}(r)$ and running coordination numbers $N_{Zr-X}(r)$ for the Zr^{4+}–X^- (X:F or Cl) pair: (*a*) $g_{Zr-X}(r)$; (*b*) $N_{Zr-X}(r)$.

The power spectra of the velocity autocorrelation functions for Zr^{4+} and F^- are shown in figure 3. The spectra for Zr^{4+} and F^- show the same tendencies. Both spectra have a peak at around 800 cm^{-1}. Thus it can be assigned to the stretching vibration Zr–F bonds. One can see that the peak frequency of this mode is independent of the anion substitutions. This is consistent with our previous experimental study in which we have reported that the frequency of the stretching vibration of Zr–F bonds is independent of Cl^- substitution in ZrF_4 glasses [20]. Both the MD and the experimental results show that Zr^{4+} ions are surrounded only by F^- ions and that very few Cl^- ions coordinate to Zr^{4+} within the substitution range 0–10 anion% of Cl^-.

Table 3 shows the distributions of the number of F^- ions which are present in the ZrF_n polyhedra. For the 0Cl system, only the polyhedra with $n = 7$ or 8 exist. However, those with $n = 6$ or 9 are also observed in the 5Cl and 10Cl systems. The network connectivity of ZrF_n polyhedra is also studied by counting the numbers of F^- ions in the corner-shared configuration and those in the edge-shared configuration. These are shown in table 3. It is found that the corner-shared F^- decreases and the edge-shared F^- increases with increasing amount of Cl^- substitution. The increase in the edge-shared F^- contributes to keep the F^- coordination number around 7.7 using a smaller amount of F^- ions.

Table 3. Anion coordination number around Zr^{4+} and the interconnectivity of ZrF_n polyhedra.

	Anion coordination number around Zr^{4+} (%)					Interconnectivity of ZrF_n polyhedra (%)	
Sample	5	6	7	8	9	Corner-shared F^-	Edge-shared F^-
0Cl	0	0	28.7	71.3	0	91	9
5Cl	0	1.8	26.0	70.4	1.8	88	12
10Cl	0.1	5.0	62.8	31.9	0.2	79	21

The distributions of F–Zr–F bond angles are shown in figure 4. The width of the peak around $\theta = 75°$ increases with increasing Cl^- substitution. F–Zr–F bond angle is distributed in a wider range as the Cl^- substitution increases.

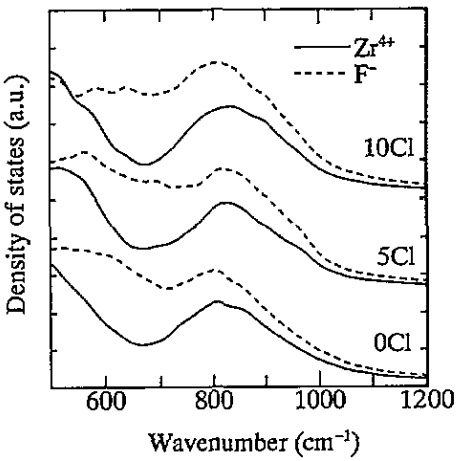

Figure 3. Power spectra of the velocity autocorrelation functions for Zr^{4+} and F^- (a.u., arbitrary units).

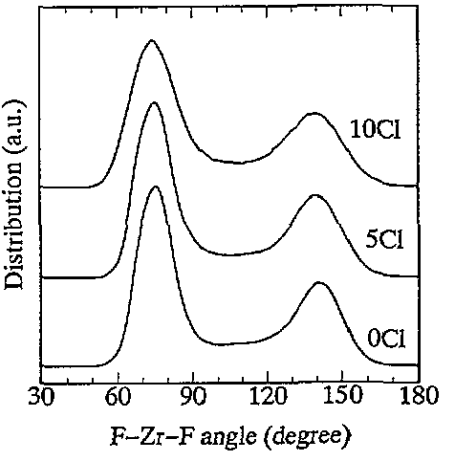

Figure 4. Distributions of F–Zr–F bond angles (a.u., arbitrary units).

From the present MD results, it is found that the average Zr^{4+}–F^- interionic distance and the average F^- coordination number around Zr^{4+} are not greatly affected by the anion substitution. However, the variation in the number of F^- in ZrF_n polyhedra and the network structures of ZrF_n polyhedra are found to be affected by the anion substitution.

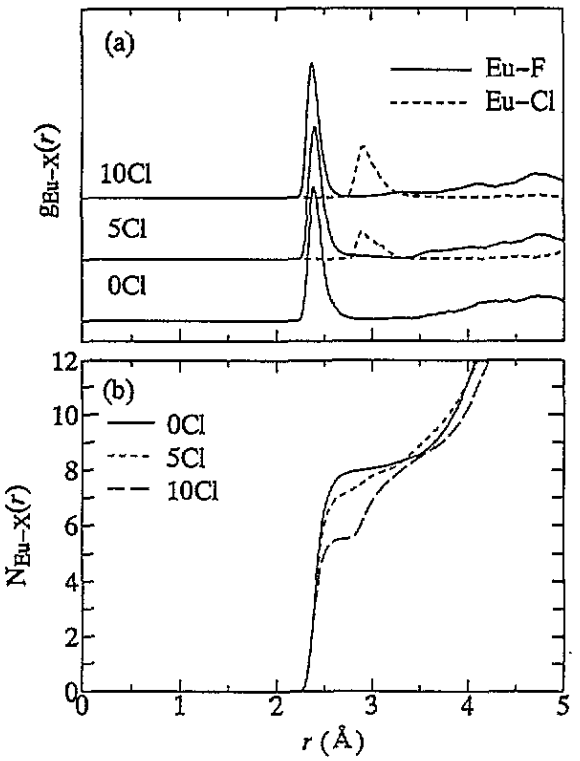

Figure 5. Pair correlation functions $g_{Eu-X}(r)$ and running coordination numbers $N_{Eu-X}(r)$ for the Eu^{3+}–X^- (X:F or Cl) pair: (*a*) $g_{Eu-X}(r)$; (*b*) $N_{Eu-X}(r)$.

3.3. Local structures around Eu^{3+}

The pair correlation functions $g_{Eu-X}(r)$ and the running coordination numbers $N_{Eu-X}(r)$ for the Eu^{3+}–X^- (X:F or Cl) pair are shown in figure 5. As can be seen from the $g_{Eu-X}(r)$ curves, the average interionic distances of the Eu^{3+}–F^- and Eu^{3+}–Cl^- pairs are 2.41 Å and 2.96 Å, respectively. These are mostly independent of the anion substitution. $N_{Eu-X}(r)$ curves for 0Cl has a clear shoulder at 2.5 Å as is seen on that of the Zr–F pair. $N_{Eu-X}(r)$ curves for 5Cl and 10Cl show two discernible shoulders at 2.5 and 3.0 Å. The former shoulder corresponds to the Eu–F pair; the latter corresponds to the Eu–Cl pair. The total anion coordination numbers around Eu^{3+} are approximately 9.5 at a distance of 3.5 Å for all glass compositions treated in this work. Figure 6 shows the distributions of coordination numbers of F^- and Cl^- around Eu^{3+}. We used the threshold distance of 3 Å for Eu–F bonds and that of 4.0 Å for Eu–Cl bonds. The average F^- coordination numbers around Eu^{3+} are 8.1, 7.4 and 5.7 for 0Cl, 5Cl and 10Cl, respectively. For the 0Cl system, the number of F^- ions in the EuF_n polyhedra is 7, 8, 9 or 10, and the principal number is 8. This result is almost consistent with the experimental data of Lucas *et al* [21] obtained from the x-ray and MD investigations on a ZB glass. For the 5Cl system, the principal F^- coordination number is also 8. However, the rate of eight-F^--coordinated Eu^{3+} is smaller than that for 0Cl system and many six-F-coordinated Eu^{3+} exist. For the 10Cl system, F^- coordination numbers around Eu^{3+} are distributed widely from 2 to 9 and the principal number of F^- around Eu^{3+} is 5. The Cl^- coordination number around Eu^{3+} for 5Cl is 0, 1 or 2; that for

10Cl is 0, 1, 2, 3, 4 or 5. The average Cl^- coordination numbers are 0.6 for 5Cl and 1.78 for 10Cl. The Cl^- coordination number increases with decreasing F^- coordination number around Eu^{3+}. All these results indicate that the substituted Cl^- coordinates to Eu^{3+}, and the coordination number of Cl^- around Eu^{3+} seems to increase proportionally with increasing amount of Cl^- substitution.

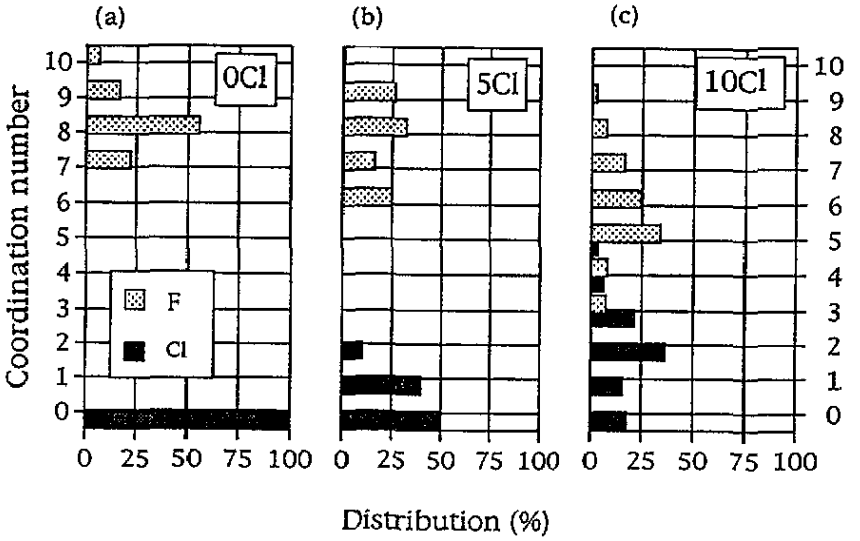

Figure 6. Distribution of the coordination number of F^- and Cl^- around Eu^{3+}: (*a*) for 0Cl; (*b*) for 5Cl; (*c*) for 10Cl.

The distribution functions of F–Eu–F bond angles in EuX_7 (X:F and/or Cl) polyhedra are shown in figure 7. The average F–Eu–F angles for the 5Cl and 10Cl systems become smaller than that for the 0Cl system in which no Cl^- ions exist in EuX_7 polyhedra. This is attributable to the fact that the ionic radius of Cl^- is larger than that of F^-.

Figure 8 shows the power spectra of the velocity autocorrelation functions for Eu^{3+}, F^- and Cl^- obtained from Fourier transformation of the velocity autocorrelation functions. A small shoulder appears for the 5Cl and 10Cl systems on the higher-energy side of the peak around 250 cm^{-1}. We have experimentally observed that the phonon energy coupled to Eu^{3+} in ZrF_4 glass systems shifts to a higher-energy region by the substitution of Cl^- for F^- [15]. The shoulder on the higher-energy side of the power spectra obtained by simulations agree with the experiments. This high-energy peak in the spectra for Eu^{3+} seems to correlate to that for Cl^-. We suppose that the existence of Cl^- produces the high-energy phonon modes around Eu^{3+}.

The local structure changes around Eu^{3+} with the anion substitution are summarized as follows.

(i) Cl^- substituted for F^- exists around Eu^{3+}, and Cl^- coordination numbers around Eu^{3+} increase in proportion to the Cl^- concentration.

(ii) The total anion coordination number around Eu^{3+} is independent of the Cl^- concentration. In other words, the F^- coordination number decreases with increasing Cl^- coordination number.

(iii) The F–Eu–F bond angle distribution shifts to a smaller-angle region.

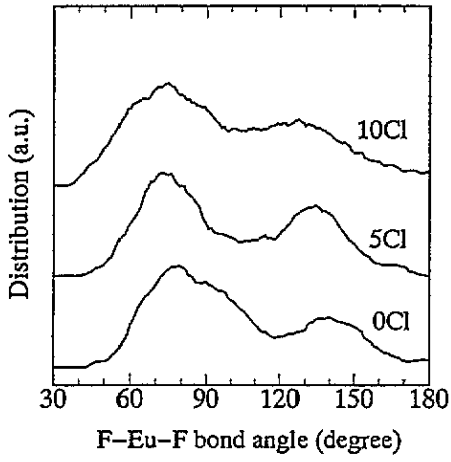

Figure 7. Distribution of F–Eu–F bond angles in EuX_7 (X:F and/or Cl) polyhedra (a.u., arbitrary units).

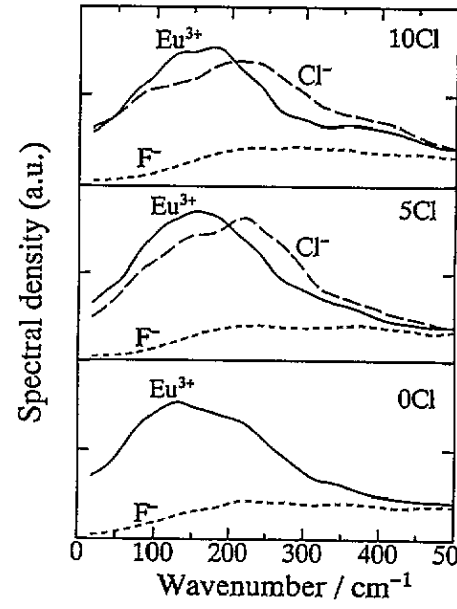

Figure 8. Power spectra of the velocity autocorrelation functions for Eu^{3+}, F^- and Cl^- (a.u., arbitrary units).

(iv) The existence of Cl^- produces the high-energy (high-frequency) phonon modes around Eu^{3+}.

3.4. Local structure around Ba^{2+}

The pair correlation functions $g_{Ba-X}(r)$ and the running coordination numbers $N_{Ba-X}(r)$ for Ba^{2+}–X^- (X:F or Cl) pair are shown in figure 9. The distribution of the Ba^{2+}–X^- interionic distance is much wider than that of Zr^{4+}–X^- or Eu^{3+}–X^-. The Cl^- coordination number around Ba^{2+} is the largest of all. Since Ba^{2+} is a network-modifying cation in the glass systems, the anions are weakly bonded to Ba^{2+} and construct BaF_nCl_m polyhedra.

The Cl^- coordination numbers around the cations increase in the order Zr^{4+}, Eu^{3+} and Ba^{2+}. This can be explained by comparing the interionic potential energies between those cations and anions. The potential curves for the cation–anion pairs are depicted in figure 10. The minima in the potential curves for cation–Cl^- pairs are shallower than for cation–F^- pairs in all cases. Thus the total potential energy increases with increasing anion substitution of Cl^- for F^-. The energy differences at the minimum of the potential curves between the cation–F^- pair and the cation–Cl^- pair are 0.88×10^{-18} J, 0.52×10^{-18} J and 0.28×10^{-18} J for Zr^{4+}, Eu^{3+} and Ba^{2+}, respectively. Thus the substituted Cl^- ions preferentially coordinate to Ba^{2+} or Eu^{3+} to keep the total potential energy lower.

4. Concluding remarks

We have carried out MD simulations for ZrF_4–BaF_2–EuF_3 glass systems to investigate changes in the local structures around glass constitutive cations with increasing amount

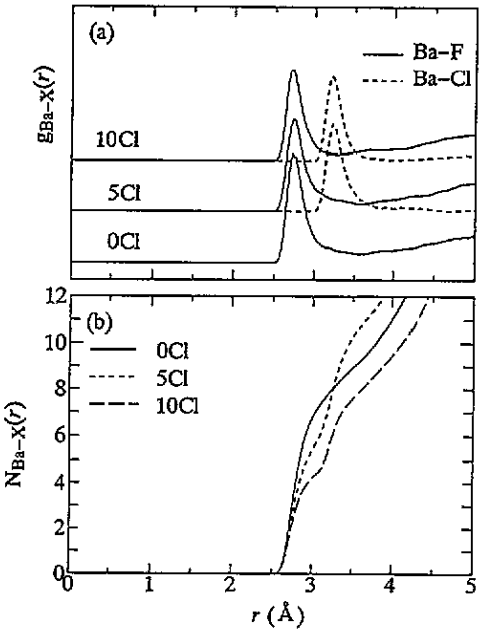

Figure 9. Pair correlation functions $g_{Ba-X}(r)$ and running coordination numbers $N_{Ba-X}(r)$ for the Ba^{2+}–X^- (X:F or Cl) pair: (*a*) $g_{Ba-X}(r)$; (*b*) $N_{Ba-X}(r)$.

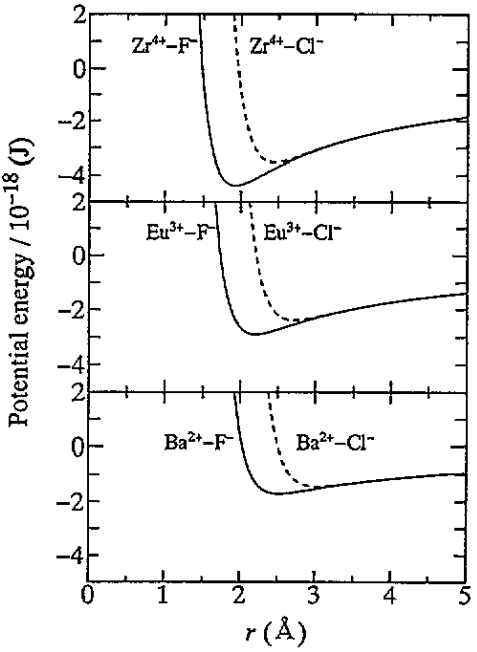

Figure 10. Potential curves for the cation–anion pairs.

of the substitution of Cl^- for F^-. Three glass compositions have been studied: 0Cl, 5Cl and 10Cl.

It is found from the present MD simulations that the F^- coordination number around Zr^{4+} is approximately 7.7 and independent of Cl^- concentration. The F^- coordination numbers around Ba^{2+} and Eu^{3+} are found to decrease with increasing Cl^- concentration. Instead of this, Cl^- coordination numbers around Ba^{2+} and Eu^{3+} increase. The total anion coordination numbers around Eu^{3+} remain unchanged. These MD results clearly show that Cl^- substituted for F^- mostly exists around the Ba^{2+} or Eu^{3+} cation. Only very few Cl^- exist around Zr^{4+} in the Cl^--substituted ZrF_4 glasses treated in the present work. The power spectra obtained by the present simulations also support this.

We have investigated also the network structures of ZrF_n polyhedra and F–Zr–F bond angle distributions. MD results show that the distribution of numbers of F^- ions in ZrF_n becomes wider as the amount of Cl^- ions increases. The F–Zr–F bond angle distribution also becomes wider with increasing Cl^- substitution.

Acknowledgments

M T would like to thank Professor K Kawamura for providing the MD code (MXDORTO) used in the present work. Part of the present calculations were carried out using the SCITEC information system at the Graduate School of Science and Technology, Kobe University. This work was supported by a grant-in-aid for scientific research 03650626 from the Ministry of Education, Science and Culture.

References

[1] Drexhage M G, Hutta J J, Suscavage M J, Mossadegh R and Moynihan C T 1985 *Mater. Sci. Forum* **6** 509
[2] Almeida R M and Mackenzie J D 1981 *J. Chem. Phys.* **74** 5954
[3] Hirao K, Todoroki S and Soga N 1992 *J. Non-Cryst. Solids* **143** 40
[4] Doel R S, Hewak D W, Jordery S, Poulain M, Baró M D and Payne D N 1993 *J. Non-Cryst. Solids* **161** 257
[5] Danger T, Koetke J, Heumann E, Huger G and Chai B H T 1994 *J. Appl. Phys.* **76** 1413
[6] Coey J M D, McEvoy A and Shafer M W 1981 *J. Non-Cryst. Solids* **43** 387
[7] Almeida R M, de Baros Marques M I and Gonçalves M C 1994 *J. Non-Cryst. Solids* **168** 144
[8] Santa-Cruz P, Auzel F, Sadoc A, Dexpert-Ghys J, Henoc P, Morin D, Hubert S and Grannec J 1993 *J. Non-Cryst. Solids* **161** 70
[9] Wang W, Chen Y and Hu T 1993 *J. Non-Cryst. Solids* **152** 172
[10] Tanabe S, Takahara K, Takahashi M and Kawamoto Y *J. Opt. Soc. Am.* B at press
[11] Adams J L, Ponçon V, Lucas J and Boulon G 1987 *J. Non-Cryst. Solids* **91** 191
[12] Todoroki S, Hirao K and Soga N 1992 *J. Non-Cryst. Solids* **143** 46
[13] Soga K, Inoue H and Makishima A 1993 *J. Lumin.* **55** 17
[14] Ogawa H, Shiraishi Y, Kawamura K and Yokokawa T 1990 *J. Non-Cryst. Solids* **119** 151
[15] Hirao K and Soga N 1985 *J. Am. Ceram. Soc.* **10** 515
[16] Kawamoto Y, Kanno R, Yokota R and Takahashi M 1993 *J. Solid State Chem.* **103** 334
[17] Yano T 1994 *Doctor's Thesis* Tokyo Institute of Technology
[18] Elyamani A, Poulain M, Saggese S J and Sigel G H Jr 1990 *J. Non-Cryst. Solids* **119** 187
[19] Ewald P P 1921 *Ann. Phys., NY* **64** 253
[20] Takahashi M, Kanno R and Kawamoto Y to be submitted
[21] Lucas J, Louër D and Angell C A 1985 *Mater. Sci. Forum* **6** 499